Detailed studies of mid-ocean ridge volcanism at the Mid-Atlantic Ridge (45N) and elsewhere

YEO, ISOBEL,ALICE,L

Appendix 9.10: Strontium Isotope Geochemistry of Zoned Plagioclase

9.10.1 Rationale

Studying the surface of an AVR informs us about its eruption styles, distribution of units, eruption timings and evolution. However, AVRs are 3D features fed by complex plumbing systems and many magma chambers. As such, it is important to attempt to constrain the processes occurring beneath the surface. Geochemistry of collected samples can provide a window into magma chamber and pre-eruption events. Comprehensive major and trace element studies are being carried out as a partner study to this thesis (at NOC, Southampton) to investigate how different hummocks are related to each other, the sources of different lava morphologies and how many magma sources have fed the eruptions that build the AVR. In addition, detailed analyses of zoned crystals provide a method to study how the magma composition is evolving before it is erupted and can shed light on processes such as magma mixing and contamination by wall rock assimilation (e.g., Davidson et al. (2007)). In this chapter I attempt to use $^{87}Sr/^{86}Sr$ ratios in zoned plagioclase to evaluate the number of crystal populations that existed in the melt, and to study the changing ratio through time as a measure of melt evolution as a result of rock wall assimilation or melt mixing.

This chapter discusses the results of Sr isotope analyses on a subset of samples and finds that the results are not reliable due to contamination of the activator and resin used in the experimental procedure. All geochemical data can be found in appendix 9.10.

9.10.2 Introduction

Strontium has four naturally occurring stable isotopes ^{84}Sr, ^{86}Sr, ^{88}Sr and the radiogenic ^{87}Sr. Strontium isotope (Sr – isotope) geochemistry is a particularly useful petrogenetic tool as the isotopic ratio of $^{87}Sr/^{86}Sr$ is not affected by partial melting or fractional crystallisation under equilibrium conditions (White and Schilling, 1978). The current bulk earth $^{87}Sr/^{86}Sr$ ratio is 0.7052, which is relatively radiogenic compared to the $^{87}Sr/^{86}Sr$ ratio for chondritic meteorites with of 0.699 (Faure, 1986). This ratio is thought to be the best approximation for early earth composition and is produced by the decay of ^{87}Rb to ^{87}Sr (Faure, 1986). Typical ratios for MORB are 0.7024 – 0.7035 (N-MORB is 0.7024 – 0.7030), although MORBs can exhibit higher ratios up to ~0.7045 (Faure, 1986; Ito et al., 1987; Schilling et al., 1983; White and Schilling, 1978; Workman and Hart, 2005). Basalts with higher ratios (~ 0.7035 – 0.7055) can be attributed to incorporation of subducted oceanic or continental crustal material into their mantle sources (Hawkesworth et al., 1979; White and Hofmann, 1982). This subducted continental material has a higher $^{87}Sr/^{86}Sr$ ratio due to hydrothermal alteration by seawater ($^{87}Sr/^{86}Sr$ ratio of 0.709) and incorporation of terrigenous sediments (variable ratios) (Faure, 1986). These basalts, called Ocean Island Basalts (OIB), are found in locations like Hawaii and the Azores, associated with mantle plumes. Elevated $^{87}Sr/^{86}Sr$ signatures (of up to 0.709 – 0.710 in the Andes) can be attributed to assimilation of continental crust (e.g. Davidson et al. (2005)).

Schilling et al. (1983) and White and Schilling (1978) present results of a comprehensive study of $^{87}Sr/^{86}Sr$ ratios in whole rock MORB along the Mid-Atlantic Ridge between 29˚N and 73˚N. They find that Mid-Atlantic Ridge basalts are characterised by typical N-MORB ratios, with the exception of three distinct, more radiogenic (higher $^{87}Sr/^{86}Sr$ ratio) areas: one associated with the Azores platform (0.70345), one at 45˚N (0.70340) and a third near the Oceanographer fracture zone at 35˚N (0.70340). The Azores maximum is associated with the Azores mantle plume, and they postulate that relic plumes may have existed beneath 35˚N and 45˚N. These raised isotopic ratios are not observed north or south of

the 45˚N area with measured ratios in basaltic glasses of 0.70285 at 49.81˚N and 0.70334 at 42.96˚N (Ito et al., 1987). Little to no geochemical variation has been noted in samples across axis (Tarney et al., 1980).

Large sections of the seafloor are metamorphosed by hydrothermal activity (Wolery and Sleep, 1976). As seawater has a higher $^{87}Sr/^{86}Sr$ ratio than either N-MORB or E-MORB sources, incorporation of seawater into magmas feeding the AVR can substantially increase the measured $^{87}Sr/^{86}Sr$ ratio. The degree of isotopic exchange depends on the water/rock ratio and the concentrations of Sr in the hydrothermal fluids (typically ~8ppm; (Faure, 1986). This process is important when we consider that the walls of magma chambers are probably composed of hydrothermally altered basalts, and that the longer magmas are stored, the more magma chamber wall rock assimilation can potentially occur, thus altering the geochemical and isotopic characteristics of the magma before eruption (e.g. Michael and Schilling (1989)). Changing Sr isotopic ratios within an evolving magma will be recorded by minerals crystallising from the melt (e.g. Hattori and Sato (1996)) and plagioclase is particularly useful for examining $^{87}Sr/^{86}Sr$ ratios from the magma as Sr is highly compatible in this phase (Ewart and Griffin, 1994; Faure, 1986).

9.10.3 Work Division

All sample preparation, micromilling, dissolution and column chemistry was done by I Yeo under the guidance of G Nowell and C McLeod at Durham University, following the procedure laid out by Harlou et al. (2009). The majority of TIMS analyses were done by I Yeo, although some were also run by S Collins and C McLeod at Durham University. ICP-MS was carried out by I Yeo and C McLeod under the guidance of C Ottley. Data analysis was done by I Yeo with help from G Nowell and further measurements to constrain potential sources of lab-derived contamination of samples were done by I Yeo, C McLeod and S Collins.

9.10.4 Methodology

9.10.4.1 Sample preparation and analysis

Micro-milled samples were analysed following the procedure detailed in Harlou et al. (2009) in the clean and ultra-clean NCIET (Northern Centre for Isotopic and Element Tracing) laboratories at Durham University. Only UpA grade aids were used in sample preparation. Appropriate (> 0.1 cm), zoned plagioclase crystals were selected from polished thick sections (100 μm) of a subset of samples. Only primary, well-preserved crystals sitting in fresh glasses (black, isotropic, away from any veining or obvious fluid flow) were analysed. Zones were then sampled by micromill following the procedure of Charlier et al. (2006). Samples were cleaned in an ultrasonic water bath in purified (MQ) water before micromilling and between each micromill of the same crystal. Drilled sample was collected in a droplet of MQ water, which was pipetted onto a pre-weighed gold foil boat. The water is then evaporated and the sample weighed before dissolution. Plagioclase separates were also picked from crushed rock samples. Four of the ten plagioclase separate samples were leached in MQ water in an ultrasonic bath for two hours prior to dissolution.

The dissolution of all samples was carried out following the methodology described in Harlou et al. (2009). After dissolution 10% aliquots were taken from the sample solution for ICP-MS analysis. The remaining sample was subsequently passed through Eichrom Sr spec resin columns (Harlou et al., 2009).

Once the Sr had been collected it was dried down and then taken up in 1.0 μl of 16N HNO_3, at which point it was ready to be run on the mass spectrometer. As described in Harlou et al. (2009), samples and standards are loaded onto outgassed Re filaments. Samples and standards (international standard NBS 987) were loaded with 1 μL of TaF_5 activator (Charlier et al., 2006). TIMS analyses were performed on a ThermoFinnigan Triton using a positive ion lens stack following Harlou et al. (2009). Rb is burned off at low currents before the current is raised to > 0.1 V to produce a measurable signal of Sr. The Sr beam strength is determined by the current through the filament (controlled by the user) and the amount of Sr in the sample. The ratio is measured 200 times in a single run and the results are averaged to give a single $^{87}Sr/^{86}Sr$ ratio for each analysed sample. Samples with higher concentrations of Sr, or which are loaded more centrally, will typically produce higher beam strengths at lower currents through the filament.

Trace element aliquots were dissolved in 500 µl of 3N HNO_3 and analysed for 25 trace elements on the ThermoElectron Element II ICP-MS at Durham University. Parameters were similar to those used by McLeod et al. (2012) and are given in Font et al. (2007).

9.10.4.2 Errors

Measured Sr isotopic ratios are processed using standard 2σ rejection criteria (Harlou et al., 2009). The reproducibility of the 21 standards (12 – 3 ng) analysed during the sample period of these analyses was 0.710260 ± 0.000015 (2 standard deviations, n = 200), and for the nine 3 ng standards (those of the 21 analysed that produce beam sizes more typical of the samples analysed) of 0.71026 ± 0.000013 (2 standard deviations, n = 200). This is in excellent agreement with the value obtained by Thirlwall (1991) of 0.710248 ± 0.000023. The mass of Sr analysed varied from 5.2 ng to 0.2 ng in the micro-milled samples and, assuming similar concentrations, probably exceeded 8 ng in the plagioclase separates. The average procedural blank (n=11) contained 15 pg Sr (± 1.6 pg), which accounts for less than 8 % of the Sr measured in the smallest sample (M119-2), less than 3 % of all but two micro-milled samples (94 %) and considerably less than 1 % of the plagioclase separates. Therefore, while the blank error is small, in some of the smallest micro-milled samples it may exceed the internal run uncertainties. This is not the case for the plagioclase separates.

Aliquotting repeatability is presented in Harlou et al. (2009) and has reproducibility of 10% or better.

9.10.5 Samples

A subset of 4 samples from two different dives was used in this initial study to test the method: JC24 -89-5, JC24-89-15, JC24-93-25 and JC24-93-31.

Sample JC24-89-5 (figure 9.10.1) is a fragment taken from the chilled margin of an exposed dyke observed in a small scarp (see figure 2.3 Q). It contains phenocrysts of well developed zoned plagioclase 0.1 – 0.5 cm in length (20 – 30% total rock), subhedral clinopyroxene (5 – 10%) and rounded olivine (<

5%), in a groundmass composed of predominantly plagioclase microlites with minor (< 2%) olivine and clinopyroxene. The glassy groundmass is fairly fresh with minor palagonite in the outer rim (0.1 mm).

Sample JC24-89-15 (figure 9.10.1) is taken from a pillowed haystack. It contains phenocrysts of zoned plagioclase 0.03 – 0.3 cm in length (15 – 20%), well developed crystals of clinopyroxene (10 – 15%), and euhedral olivine (5 %) in a glassy groundmass containing microlites of the same minerals as the phenocrysts. The glass exhibits small degrees of devitrification and palagonite visible only on the outermost 1 cm of the hand specimen.

Sample JC24-93-25 (figure 9.10.1) is a section of a pillow lava. It contains phenocrysts of well developed zoned plagioclase 0.2 – 0.5 cm in length (30 – 40%), rounded olivines (5 – 10%) and euhedral clinopyroxene (5 – 10%). The groundmass is glassy with microlites of the same phases as the phenocrysts and while the outer few cm appears devitrified in hand specimen, the centre appears unaltered.

Sample JC24-93-31 (figure 9.10.1) is a small section of pillow crust taken from a haystack. It contains phenocrysts of well developed, zoned plagioclase 0.2 – 0.5 cm in length (20-30%), subhedral olivine (5 – 10%) and clinopyroxene (5 – 10%) in an entirely glassy groundmass with no microlites. Devitrification is extensive and extends for several cm into the specimen from either side, although a thin band (~ 1.5 cm) of darker glassy material remains unaltered (devitrification is observed in small, isolated patches) in the centre of the sample.

Three crystals (three cores and rims) were analysed from sample JC24-89-5, 2 crystals (two cores and rims) were analysed from sample JC24-89-15, four crystals (four cores and rims) were analysed from sample JC24-93-25 and three crystals (three cores and rims plus one intermediate zone, M117-5) were analysed from sample JC24-93-31. Additionally four drilled glasses were analysed from sample JC24-93-31 and five plagioclase separates were analysed each from samples JC24-93-31 and JC24-89-15.

9.10.6 Data

$^{87}Sr/^{86}Sr$ data for all micro-milled samples (crystals and glasses) is shown in figure 9.10.2 and table 9.10.1. All samples except one glass exceeded the measured White and Schilling (1979) ratios. With the exception of two rims, all the micro-milled crystals have $^{87}Sr/^{86}Sr$ ratios which exceed 0.705, many lying above even the OIB range (0.703 – 0.7055). The three glasses that were analysed have lower $^{87}Sr/^{86}Sr$ ratios, with an average of 0.70351, although two of the samples still lie above the White and Schilling (1978) ratios, which were measured in the 45°N area.

$^{87}Sr/^{86}Sr$ ratio data for the plagioclase separates is shown in figure 9.10.3. The average $^{87}Sr/^{86}Sr$ ratio for 5 plagioclases from sample JC24-89-15 is 0.703048 $\pm$ 0.000043 and for the five crystals from JC24-93-31 it is 0.703155 $\pm$ 0.000202. Both these $^{87}Sr/^{86}Sr$ ratios are lower than the $^{87}Sr/^{86}Sr$ ratio measured in any of the zones of plagioclases in the corresponding samples. The zoned plagioclase results are surprising, and much too high to be realistic. Possible explanations may include alteration, analytical errors or contamination (discussed in 9.10.7).

The trace element data are shown in figure 9.10.4. The left hand panel shows all the trace element data for the plagioclase zones and glasses normalized to primitive mantle. The glasses display a slightly different trend to the plagioclase crystals. The right hand panel shows the trace element patterns for hydrothermal fluids from two nearby hydrothermal fields (Snake Pit hydrothermal field at 23°N on the Mid-Atlantic Ridge and TAG hydrothermal field at 26°N on the Mid-Atlantic Ridge) and normal seawater from the Snake Pit area from Mitra et al. (1994).

9.10.7 Discussion

9.10.7.1 Are these results realistic?

The $^{87}Sr/^{86}Sr$ isotopic values range from 0.7035 – 0.7125 for the micromilled crystal zones, from 0.7035 – 0.7040 for the micro-milled glasses, and from 0.7028 – 0.7040 in the plagioclase separates. As the plagioclase separates are from the same samples as the micro-milled samples the values should be comparable. As MORB typically has $^{87}Sr/^{86}Sr$ isotopic ratios < 0.704, the plagioclase separate ratios are

more likely to be correct and the micro-milled zoned plagioclase isotopic values over ~0.704 are unlikely to be real. Ratios greater than 0.70550 (above which most of our samples lie (figure 9.10.2)) are typically associated with volcanic arc settings or the involvement of continental crust and there is no such mechanism currently identified that could produce them at a mid-ocean ridge setting (Faure, 1986; Wilson, 1989). Values also lie way above previously measured $^{87}Sr/^{86}Sr$ ratios in the 45°N area (White and Schilling, 1978) and above those typical of the Mid-Atlantic Ridge and MORB (Faure, 1986; Ito et al., 1987; Workman and Hart, 2005), even where basalts display distinct hot-spot anomalies (Dixon et al., 2002). The glasses from sample JC24-93-31 also display slightly elevated $^{87}Sr/^{86}Sr$ isotopic ratios, but are much closer to those measured by White and Schilling (1978) and lie within reasonable bounds for E-MORB (0.7030 – 0.7045).

The plagioclase crystal separates were run to compare the isotopic ratios of the micro-milled, zoned plagioclases to those of whole crystals. These samples were much larger than any of the micro-milled samples and when analysed gave $^{87}Sr/^{86}Sr$ ratios that are much more typical of MORB values. These plagioclases were taken from samples JC24-93-31 and JC24-89-15, and the $^{87}Sr/^{86}Sr$ isotopic ratios measured from the separates were far lower than any measured in micromilled crystals from either of those samples (cores or rims) and could not have been produced by any core/rim combination. This further indicates that the measured $^{87}Sr/^{86}Sr$ ratios from the micro-milled plagioclase zones are unreliable. The rest of this chapter will deal with the causes of these anomalous results and the likely causes and results of analytical and/or methodological errors.

9.10.7.2 An explanation of the results

The only way to elevate $^{87}Sr/^{86}Sr$ ratios beyond a reasonable MORB range is through analytical error or by contaminating the samples. As we do not see the same high ratios for the plagioclase separates, which were analysed the same way, it is unlikely to be analytical error that is responsible for the raised ratios, and therefore the most likely cause is contamination. Some variation may be caused by low count numbers on samples which ran for low numbers of counts.

Geologically, contamination may occur as a result of seawater interaction, however crystals were deliberately chosen because they looked fresh and no measurable difference was observed between the

ultrasonically cleaned and uncleaned plagioclase separates. Additionally, seawater has a $^{87}Sr/^{86}Sr$ ratio of 0.709 (so cannot account for the two isotopic ratios higher than 0.709 observed in crystals A and B; figure 9.10.2) and typically only alters the isotopic ratios by a few percent where samples look fresh from petrography (Hart et al., 1974). Contamination from sources other than seawater and hydrothermal fluids is supported by the trace element concentrations (figure 9.10.4). Seawater contains much lower concentrations of Sr than the plagioclase crystals and therefore a significant amount of seawater would need to be flushed through the samples for it to substantially alter the $^{87}Sr/^{86}Sr$ isotopic ratios. Hydrothermal fluids, such as those from Snake Pit and TAG (figure 9.10.4) contain higher concentrations of the analysed trace elements than normal seawater, however no relationship exists between the trace element pattern associated with these fluids and those measured from the micro-milled samples. Notably, the hydrothermal fluids show a large Eu anomaly, which is not reflected by the Eu signature of most of the micro-milled samples.

Alternatively there may be a contamination at some point in sample preparation. If this is the case then the effect would be stronger the smaller the sample and the lower the amount of Sr within it, because there would be fewer correct measurements from the sample relative to the incorrect measurements from the contaminant. Figure 9.10.5 shows two plots, one of sample mass against $^{87}Sr/^{86}Sr$ ratio and one of the beam strength (representative of how well the sample ran and hence the result reliability) against $^{87}Sr/^{86}Sr$ ratio. Both plots show a very weak correlation between small sample masses (and therefore samples running poorly) and raised $^{87}Sr/^{86}Sr$ ratios, although these relationships are not statistically significant. The lack of a clear relationship may be due to varying contamination affect, and/or to analytical artifacts, as analyses with low counts are very unreliable.

Contamination may be occurring at any stage, however only UPA acids are used and the bottles are changed regularly, hence the same stock acids were not used during preparation of all the zoned plagioclase samples (which were micro-milled, dissolved and put through columns in three batches: M117, M118 and M119). However, the resin used in the columns and the activator used when loading samples for mass spectrometry are not changed as regularly, due to the small volumes used. Therefore the same stock supply was used for all the batches analysed, making them the most likely contaminants for the whole sample suite. To test this, six TaF_5 activator and two column resin blanks were run in the mass spectrometer. The data are shown in figure 9.10.6 and in table 9.10.1.

All but one sample ran and gave a value for $^{87}Sr/^{86}Sr$ above 0.709 (figure 9.10.6). None of the resin or activator samples ran to completion, with most only lasting for ~25% of the total analysis time (50/200 counts), although one ran for 58% (115/200 counts) of the duration of the analysis, suggesting that Sr concentrations were low (trace elements were not measured for these samples). Both the activator and resin required large currents to be run through the filament (> 2800 mA), again suggesting low Sr concentrations. Unexpectedly, despite being samples of the same material activator sample A4 is different outside of error from A1, A2 and A5. It is possible the sample A4 was accidentally contaminated elsewhere or that a larger proportion of the contaminant, possibly a particle of dust, was collected by the pipette during loading. Alternatively this could again be an analytical artifact, as these samples all ran for low a low number of counts. The activator did not show the same $^{87}Sr/^{86}Sr$ ratio as the NBS987 standard (measured as 0.710260 $\pm$ 0.000015 during these analyses) used to standardise the JC24 samples, despite this being a likely source of contamination as both are used in loading, where they are pipetted onto the filament. During this process it would be easy to 'double dip' the pipette tip, contaminating the activator with the standard. This could be because it is not to be the main or only cause of the contamination, or could be due to internal run uncertainties due to the low counts recorded during analysis of the activator and resin samples.

Activator was run with the resin blanks, although both the resin samples produced lower $^{87}Sr/^{86}Sr$ ratio values suggesting that the resin ran with a lower $^{87}Sr/^{86}Sr$ ratio than that of the activator. Additionally the two resin samples, R1 and R2, ran for the longest of all of the resin and activator samples analysed, lasting for 57 and 115 counts (of 200) respectively and also produced the highest beam strengths (0.37 and 0.27 V respectively). This suggests that the combination of both the activator and resin contained more Sr than was present in the activator alone, and therefore that both the resin and the activator contain Sr and are potential contaminants.

Both the activator and the resin required high currents through the filament to run, neither produced high beam strengths and neither ran to completion. Therefore, the effect of their individual $^{87}Sr/^{86}Sr$ ratios would be negligible for a large sample running at a high beam strength for the entire 200 count analysis. As such they are likely to have had less of an effect on the glass samples and very little (if any at all) on the plagioclase separates. However, the micro-milled zoned plagioclase samples were typically smaller

and ran at lower beam strengths, even with large currents through the filament. This meant that during the run, the current through the filament was consistently > 2800 mA. Additionally, 14 of the 24 samples run (excluding M118-2, which failed to run entirely) did not run to completion, with the worst runs (M117-5 and M118-10) only lasting for 61 and 110 counts respectively (table 9.10.1). Additionally both ran with low beam strengths averaging 0.04V and 0.13V respectively. Both these samples produced anomalously high $^{87}Sr/^{86}Sr$ ratios (M117-5 produced the highest $^{87}Sr/^{86}Sr$ ratio measured). Figure 9.10.7 shows the number of counts a sample ran for against the measured $^{87}Sr/^{86}Sr$ ratio. As shown in figure 9.10.5, there again appears to be a very rough relationship between the two (R^2 value of 0.205 for a linear trendline) although, high ratios are measured for samples that also ran to completion.

It therefore seems that it was a combination of small sample size (and therefore low beam strength) and running for less than 200 counts that was responsible for the larger effect the contamination had on the micro-milled zoned plagioclase $^{87}Sr/^{86}Sr$ ratios. Different samples could potentially have different proportions of contamination from the resin (as a result of how well the bottle was shaken, the location of the pipette tip when the resin was taken up and the different column frit paper positioning) and are probably loaded with slightly variable amounts of activator, which will vary the amount of contaminant on each loaded filament. Variable loading and sample pick up from the beaker will also control how much of an effect the contaminant has on the final $^{87}Sr/^{86}Sr$ ratio. Further contamination may have occurred from seawater interaction, and may account for the smaller variations in the plagioclase separate samples and the glass, however this effect is small as the freshest samples (little or no petrographic evidence of alteration was visible) were used and the concentration of Sr in seawater is low enough to require a very large volume of seawater to have interacted with the sample.

9.10.8 Conclusions

Measured $^{87}Sr/^{86}Sr$ ratios in the micro-milled zoned plagioclases are unlikely to be the result of any naturally occurring process and are almost certainly due to contamination of the sample. The contaminant appears to have more of an effect on small samples which did not run as well on the mass spectrometer (low voltages and not running to completion). The resin and the activator were both used in the preparation of all the samples unlike the acids which are changed regularly. Both the column resin and the activator used in sample preparation and loading were found to contain Sr and ran on the mass

spectrometer with $^{87}Sr/^{86}Sr$ ratios between 0.709500 and 0.711500. Voltages were low and none of the activator or resin samples ran to completion, however this was also the case for a number of the zoned plagioclase samples, many of which also did not run to completion and ran with low beam strengths. The glasses ran better and in general had slightly higher masses and therefore larger amounts of Sr, which probably lessened the effect of contamination.

Plagioclase separates were not similarly contaminated, probably because the sample masses were much larger than in the micro-milled samples. All but one sample lay within typical MORB values, and all of those from sample JC24-89-15 and half of the samples from JC24-93-31 showed slight enrichment. Small variations in the measured $^{87}Sr/^{86}Sr$ ratios may be due to smaller contamination effects or seawater contamination. Despite this, all but one of the crystal separate $^{87}Sr/^{86}Sr$ ratios measured lie below the White and Schilling (1978) values, suggesting that perhaps elevated $^{87}Sr/^{86}Sr$ ratios are not typical of the whole segment. The plagioclase separates had lower $^{87}Sr/^{86}Sr$ ratios than the glasses from the same sample, possibly because the glasses are more easily contaminated by seawater interaction, or because the composition of the melt changed after the plagioclase crystallised but prior to eruption. Further uncontaminated studies of $^{87}Sr/^{86}Sr$ compositional zoning are needed to test this.

9.10.9 References

Charlier, B.L.A., Ginibre, C., Morgan, D., Nowell, G.M., Pearson, D.G., Davidson, J.P., and Ottley, C.J., 2006, Methods for the microsampling and high-precision analysis of strontium and rubidium isotopes at single crystal scale for petrological and geochronological applications: Chemical Geology, v. 232, p. 114-133.

Davidson, J.P., Hora, J.M., Garrison, J.M., and Dungan, M.A., 2005, Crustal forensics in arc magmas: Journal of Volcanology and Geothermal Research, v. 140, p. 157-170.

Davidson, J.P., Morgan, D.J., and Charlier, B.L.A., 2007, Isotopic Microsampling of Magmatic Rocks: Elements, v. 3, p. 253-259.

Dixon, J.E., Leist, L., Langmuir, C., and Schilling, J.-G., 2002, Recycled dehydrated lithosphere observed in plume-influenced mid-ocean-ridge basalt: Nature, v. 420, p. 385-389.

Ewart, A., and Griffin, W.L., 1994, Application of proton-microprobe data to trace-element partitioning in volcanic rocks: Chemical Geology, v. 117, p. 251-284.

Faure, G., 1986, Principles of Isotope Geology: New York, John Wiley and Sons, 589 p.

Font, L., Nowell, G.M., Graham Pearson, D., Ottley, C.J., and Willis, S.G., 2007, Sr isotope analysis of bird feathers by TIMS: a tool to trace bird migration paths and breeding sites: Journal of Analytical Atomic Spectrometry, v. 22, p. 513-522.

Harlou, R., Pearson, D.G., Nowell, G.M., Ottley, C.J., and Davidson, J.P., 2009, Combined Sr isotope and trace element analysis of melt inclusions at sub-ng levels using micro-milling, TIMS and ICPMS: Chemical Geology, v. 260, p. 254-268.

Hart, S.R., Erlank, A.J., and Kable, E.J.D., 1974, Sea floor basalt alteration: Some chemical and Sr isotopic effects: Contributions to Mineralogy and Petrology, v. 44, p. 219-230.

Hattori, K., and Sato, H., 1996, Magma evolution recorded in plagioclase zoning in 1991 Pinatubo eruption products american mineralogist, v. 81.

Hawkesworth, C.J., Norry, M.J., Roddick, J.C., and Vollmer, R., 1979, 143Nd/144Nd and 87Sr/86Sr ratios from the Azores and their significance in LIL-element enriched mantle: Nature, v. 280, p. 28-31.

Ito, E., White, W.M., and Göpel, C., 1987, The O, Sr, Nd and Pb isotope geochemistry of MORB: Chemical Geology, v. 62, p. 157-176.

McLeod, C.L., Davidson, J.P., Nowell, G.M., and de Silva, S.L., 2012, Disequilibrium melting during crustal anatexis and implications for modeling open magmatic systems: Geology.

Michael, P.J., and Schilling, J.-G., 1989, Chlorine in mid-ocean ridge magmas: Evidence for assimilation of seawater-influenced components: Geochimica et Cosmochimica Acta, v. 53, p. 3131-3143.

Mitra, A., Elderfield, H., and Greacer, M.J., 1994, Rare earth elements in submarine hydrothermal fluids and plumes from the Mid-Atlantic Ridge: Marine Chemistry, v. 46, p. 217 - 235.

Schilling, J.G., Zajac, M., Evans, R., Johnston, T., White, W., Devine, J.D., and Kingsley, R., 1983, Petrologic and geochemical variations along the Mid-Atlantic Ridge from 29 degrees N to 73 degrees N: American Journal of Science, v. 283, p. 510-586.

Tarney, J., Wood, D.A., Saunders, A.D., Cann, J.R., and Varet, J., 1980, Nature of Mantle Heterogeneity in the North Atlantic: Evidence from Deep Sea Drilling: Philosophical Transactions of the Royal Society of London. Series A, Mathematical and Physical Sciences, v. 297, p. 179-202.

Thirlwall, M.F., 1991, Long-term reproducibility of multicollector Sr and Nd isotope ratio analysis: Chemical Geology: Isotope Geoscience section, v. 94, p. 85-104.

White, W.M., and Hofmann, A.W., 1982, Sr and Nd isotope geochemistry of oceanic basalts and mantle evolution: Nature, v. 296, p. 821-825.

White, W.M., and Schilling, J.-G., 1978, The nature and origin of geochemical variation in Mid-Atlantic Ridge basalts from the Central North Atlantic: Geochimica et Cosmochimica Acta, v. 42, p. 1501-1516.

Wilson, M., 1989, Igneous Petrogenesis: London, Unwin Hyman.

Wolery, T.J., and Sleep, N.H., 1976, Hydrothermal Circulation and Geochemical Flux at Mid-Ocean Ridges: The Journal of Geology, v. 84, p. 249-275.

Workman, R.K., and Hart, S.R., 2005, Major and trace element composition of the depleted MORB mantle (DMM): Earth and Planetary Science Letters, v. 231, p. 53-72.

9.10.10 Figures

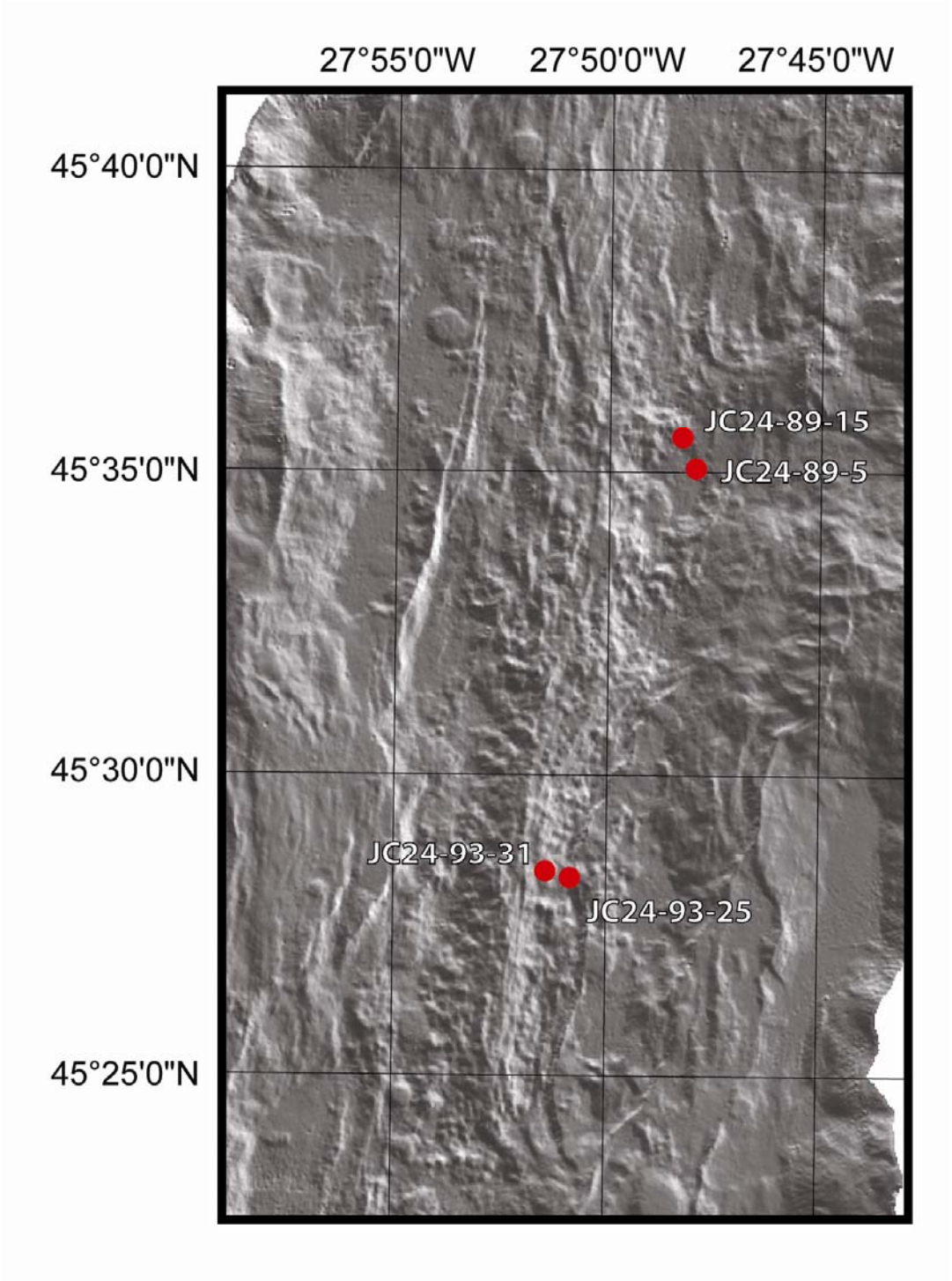

Figure 9.10.1: Sample locations on hillshaded bathymetry.

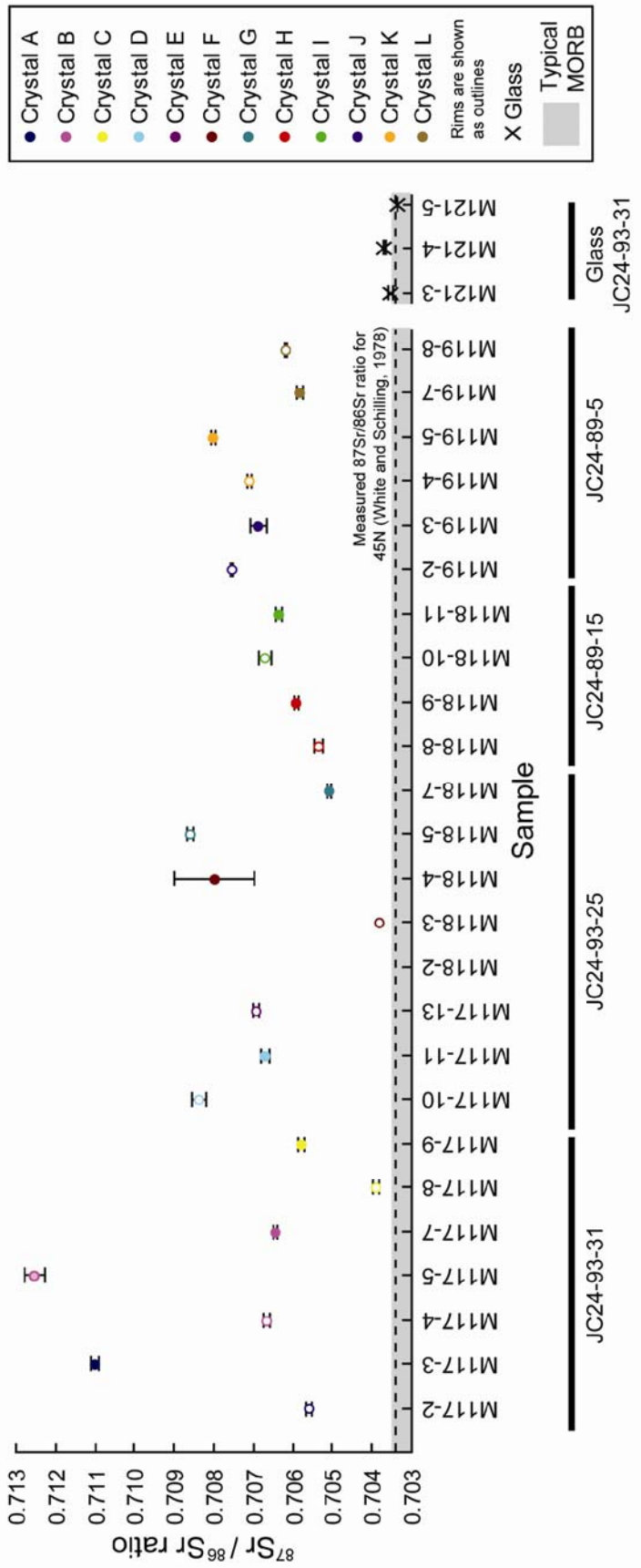

Figure 9.10.2: Analysed $^{87}Sr/^{86}Sr$ ratios for the cores and rims of micro-milled crystals. Crystals A, B, C are from sample JC24-93-31, crystals D, E, F, G from sample JC24-93-25, crystals H, I, from sample JC24-89-15 and crystals J, K, L from sample JC24-89-5. Cores are shown by solid symbols and rims are shown by outlines, The only intermediate zone is shown by a solid outline and pale coloured centre. All glasses micro-milled were from sample JC24-93-31 and are shown by black crosses. The dashed line represents the measured $^{87}Sr/^{86}Sr$ ratio for samples from 45°N measured by White and Schilling (1978). The grey area shows the normal values from $^{87}Sr/^{86}Sr$ ratios in MORB. Error bars are 2 standard deviations.

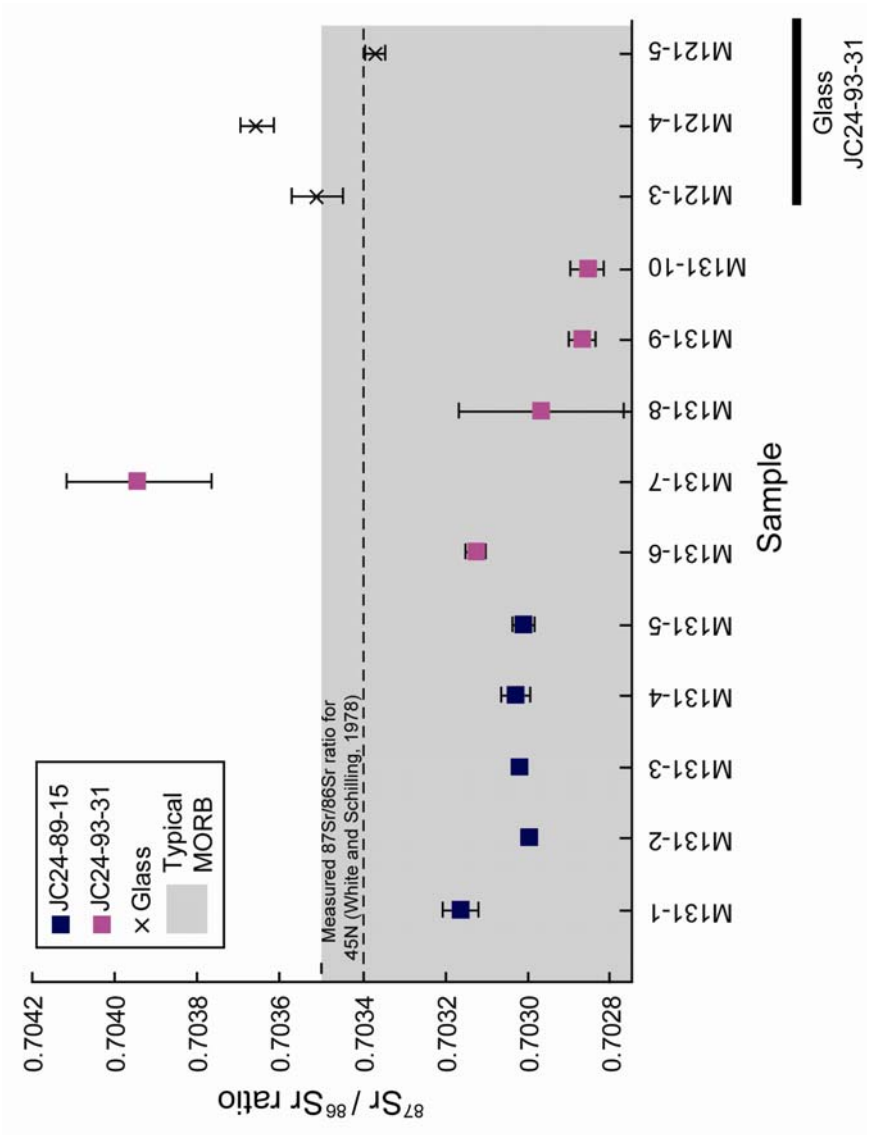

Figure 9.10.3: Analysed $^{87}Sr/^{86}Sr$ ratios for whole plagioclase crystal separates (and micro-milled glasses as shown in figure 6.2). The dashed line represents the measured $^{87}Sr/^{86}Sr$ ratio for samples from 45°N measured by White and Schilling (1978). The grey area shows the normal values from $^{87}Sr/^{86}Sr$ ratios in MORB. Error bars are 2 standard deviations. M131-1, M131-2, M131-6 and M131-7 were cleaned in an ultrasonic bath in MQ for 2 hours before dissolution. M131-7 was the only sample that ran with a beam strength less than 0.5 V.

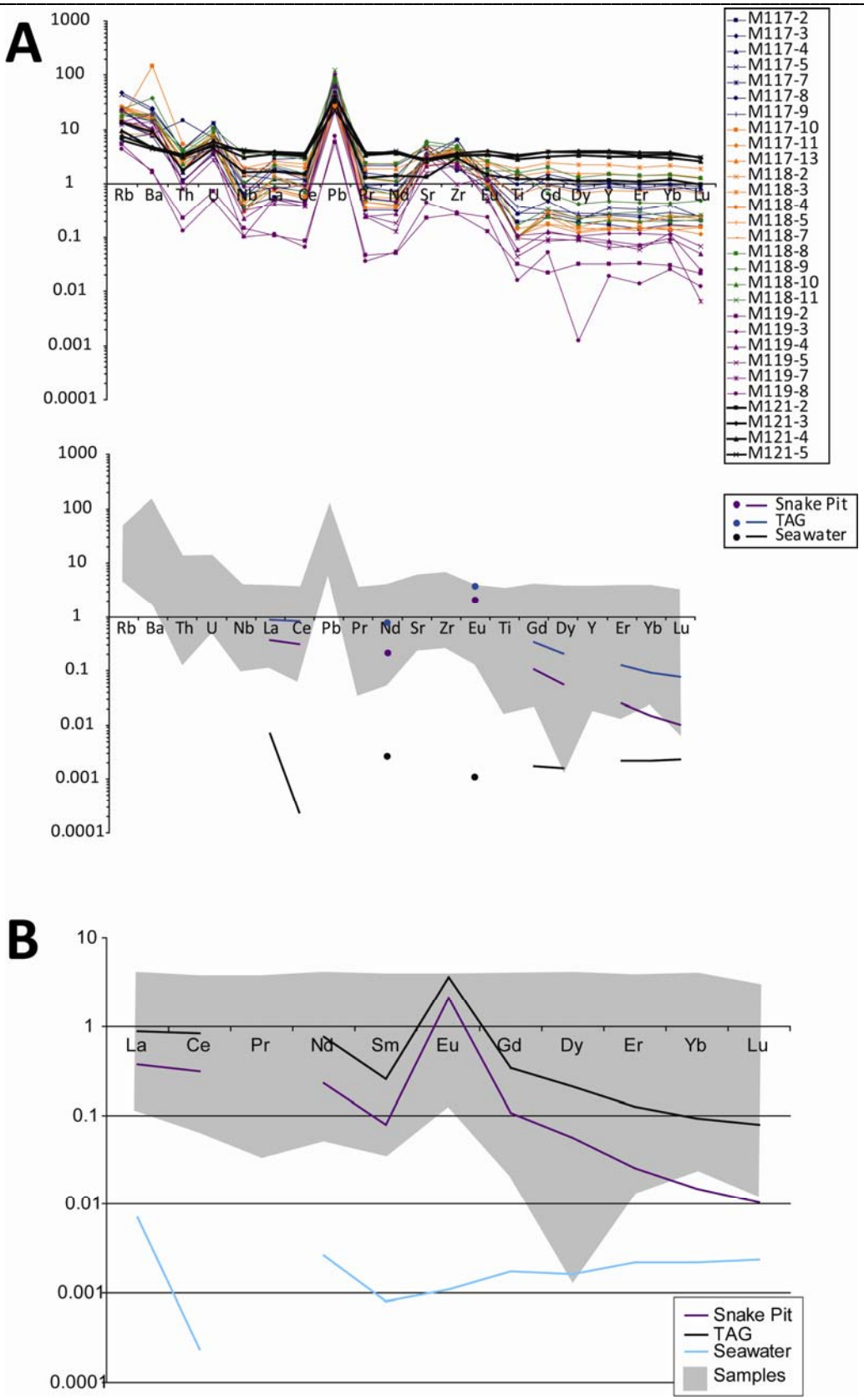

Figure 9.10.4: A) Measured trace elements normalised to primitive mantle. The upper panel shows all the samples (colour coded) and glasses (thicker black lines) measured. The single low Dy value in sample M119-8 is probably an anomaly. The lower panel shows the trace element patterns from hydrothermal fluids from Snake Pit (23˚N MAR) and TAG (26˚N MAR) hydrothermal fluids and normal seawater from the Snake Pit area (Mitra et al., 1994). The grey area is the envelope from the sample trace elements in the left hand panel. B) Shows the rare earth elements from the above plot. The envelope of the measured data is shown in grey with the hydrothermal and seawater values as a comparison.

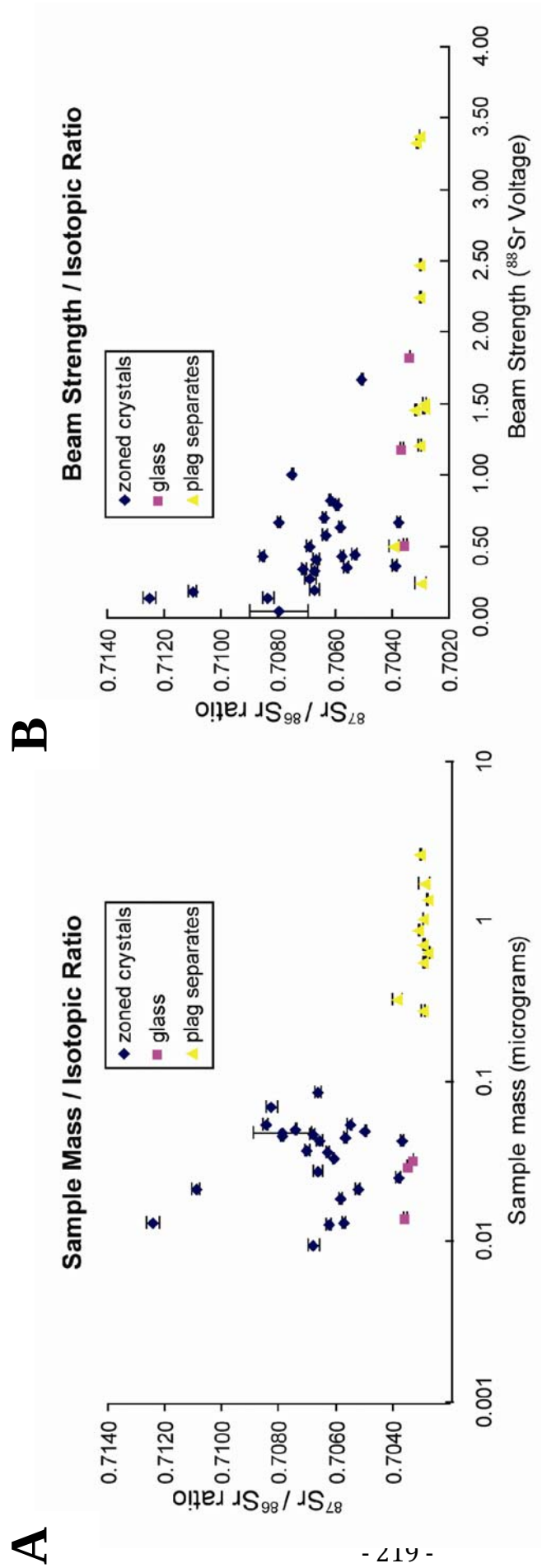

Figure 9.10.5: Analysed ^{87}Sr /^{86}Sr ratios for the zoned crystals (blue diamonds), JC24-93-31 glasses (pink squares) and plagioclase separates (yellow triangles). The graph A shows isotopic ratio plotted against sample mass. There appears to be a rough correlation between lower sample mass and higher, more scattered $^{87}Sr/^{86}Sr$ ratios. Graph B shows the beam strength samples ran at (indicative of how well they ran on the mass spectrometer) against $^{87}Sr/^{86}Sr$ isotopic ratios. Again there appears to be a correlation between sample running at higher beam strengths (well) and lower $^{87}Sr/^{86}Sr$ isotopic ratio, although this trend is not seen in the plagioclase separates. Error bars are two standard deviations. Logarithmic trend lines can be fitted to both graphs with R^2 values of 0.36 and 0.47 respectively.

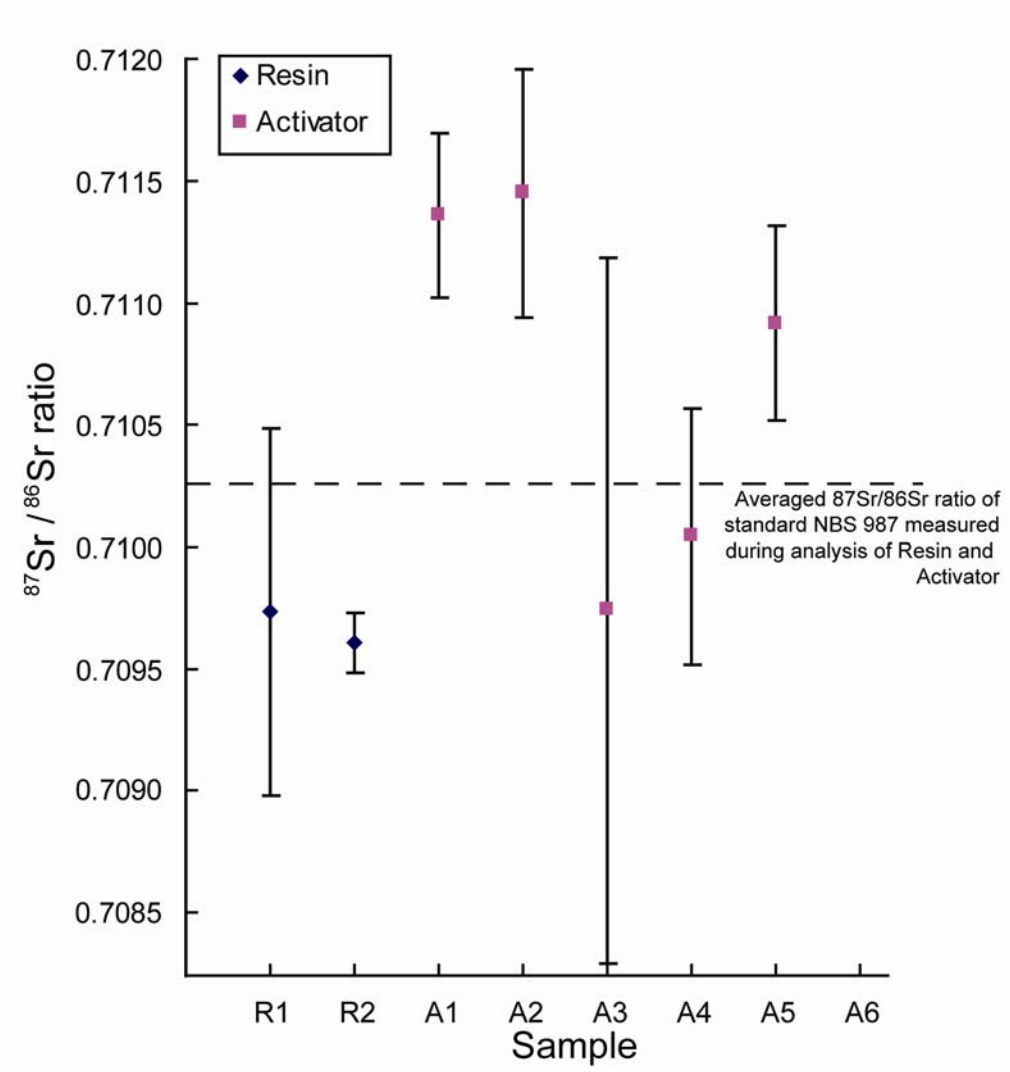

Figure 9.10.6: $^{87}Sr/^{86}Sr$ ratios measured for blanks of column resin (blue diamonds) and TaF_5 loading activator (pink squares). Only one sample (A6) did not run at all. None of the other samples ran to completion as typically the beam died ~25% of the way through the analysis i.e. at 50 counts (with the exception of R2 which ran for 66% of the total analysis time). The dashed line shows the averaged $^{87}Sr/^{86}Sr$ ratio of the NBS 987 standard as measured during analyses. Error bars are two standard deviations.

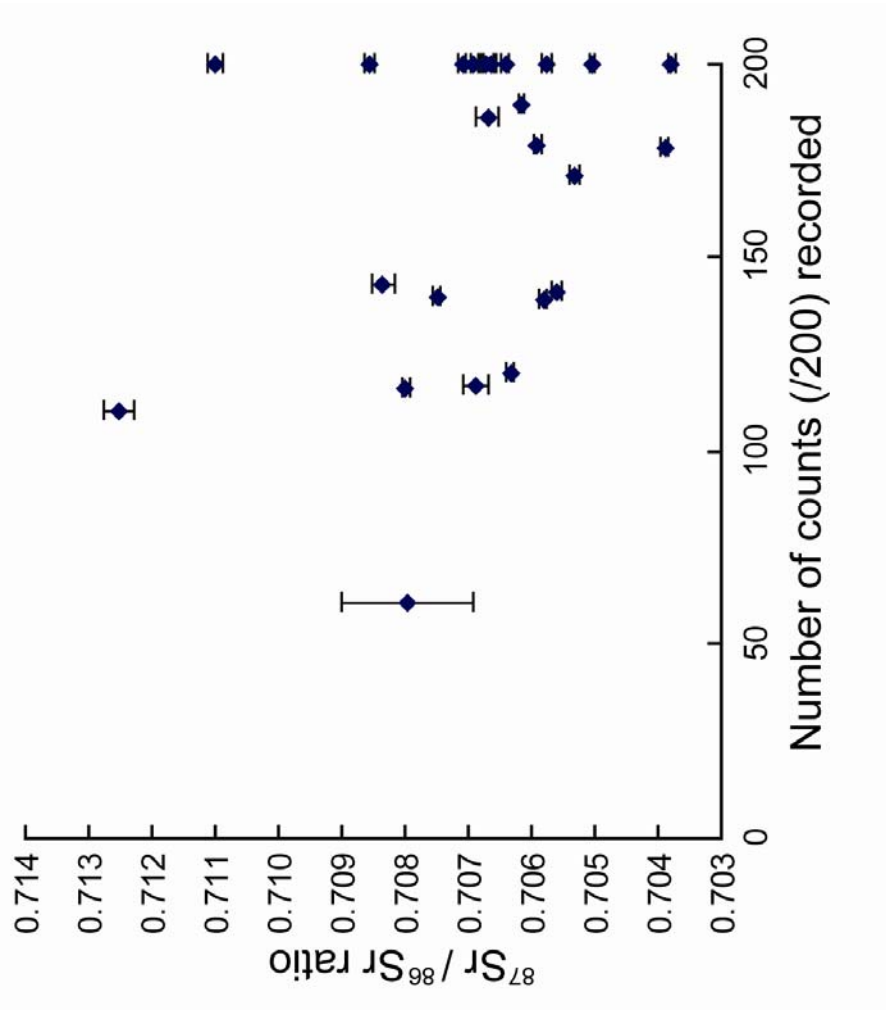

Figure 9.10.7: Analysed $^{87}Sr/^{86}Sr$ ratios for the zoned crystals plotted against the number of counts the sample ran for. Error bars are two standard deviations.

	Sample name	Ratio	2σ	88Sr (V) (beam strength)	Counts
Plagioclase zones	M117-2	0.705593	0.000082	0.35	135/141
	M117-3	0.711003	0.000126	0.18	191/200
	M117-4	0.706656	0.000096	0.41	191/200
	M117-5	0.712532	0.000244	0.13	103/110
	M117-7	0.706406	0.000058	0.70	186/200
	M117-8	0.703897	0.000076	0.36	172/178
	M117-9	0.705759	0.000062	0.43	189/200
	M117-10	0.708347	0.000184	0.13	136/143
	M117-11	0.706706	0.000108	0.33	184/200
	M117-13	0.706908	0.000071	0.49	192/200
	M118-2				FAILED
	M118-3	0.703785	0.000053	0.67	186/200
	M118-4	0.707973	0.001043	0.04	60/61
	M118-5	0.708553	0.000077	0.42	192/200
	M118-7	0.705053	0.000034	1.67	188/200
	M118-8	0.705324	0.000090	0.44	120/171
	M118-9	0.705913	0.000054	0.79	167/179
	M118-10	0.706696	0.000170	0.19	110/186
	M118-11	0.706337	0.000074	0.58	113/120
	M119-2	0.707496	0.000048	1.00	132/140
	M119-3	0.706875	0.000212	0.27	111/117
	M119-4	0.707100	0.000069	0.34	200/200
	M119-5	0.707994	0.000062	0.67	115/116
	M119-7	0.705817	0.000068	0.63	128/139
	M119-8	0.706170	0.000037	0.82	189/189
Glasses	M121-2	-	-	-	FAILED
	M121-3	0.703512	0.000062	0.50	181/181
	M121-4	0.703659	0.000042	1.18	145/152
	M121-5	0.703368	0.000025	1.83	186/200
Plagioclase separates	M131-1	0.703168	4.31E-05	1.45	192/200
	M131-2	0.703001	1.6E-05	2.24	192/200
	M131-3	0.703025	1.59E-05	3.37	186/200
	M131-4	0.703031	3.71E-05	1.21	186/200
	M131-5	0.703013	2.68E-05	2.47	190/200
	M131-6	0.703127	2.38E-05	3.32	187/200
	M131-7	0.703949	0.000176	0.5	115/148
	M131-8	0.702970	0.000202	0.24	115/197
	M131-9	0.702872	3.04E-05	1.46	188/200
	M131-10	0.702857	3.99E-05	1.5	188/200
Tests	resin	0.709737	0.00075	0.37	56/57
	resin	0.709613	0.000124	0.27	112/115
	activator	0.711363	0.000328	0.15	39/42
	activator	0.711453	0.000504	0.12	38/41
	activator	0.709741	0.00145	0.06	5/5
	activator	0.710047	0.000528	0.09	48/50
	activator	0.710918	0.000402	0.23	34/36
	activator	-	-	-	FAILED

Table 9.10.1: Sample names, ratios, errors, beam strength and runs (out of a maximum possible 200)